DNA Nanotechnology

DOI: 10.1002/anie.200906225

A Route to Scale Up DNA Origami Using DNA Tiles as Folding Staples**

Zhao Zhao, Hao Yan, and Yan Liu**

DNA-based molecular self-assembly offers an efficient route to fabricate nanostructures of increasing complexity.[1] Recently, progress in structural DNA nanotechnology has demonstrated that DNA tiles consisting of branched DNA junction motifs can be used as versatile building blocks for programmable construction of two- and three-dimensional structures with custom-designed surface patterns.[2–4] These nanostructures can be used as templates to organize proteins and nanoparticles into rationally designed patterns.[5–16] An important milestone for the advance of structural DNA nanotechnology was the development of a DNA nanostructure folding strategy, called scaffolded DNA origami, which was achieved by Rothemund.[17] In this technique, a long single-stranded viral genome (M13 phage) serving as a scaffold is arranged in a 2D plane following a designated folding path, and hundreds of short oligonucleotides, termed staple strands, hybridize with the scaffold strand through complementary base pairing to form many branched DNA junctions between adjacent helices. The staple strands assist the folding of the scaffold strand into planar 2D arrays with custom-designed shapes defined by the initial scaffold folding path. Recently, the concept of DNA origami has been applied to engineer a series of 3D DNA nanostructures with a broad range of geometric complexities,[18–23] thus further showing that DNA is one of the most promising materials to achieve highly programmable self-assembling systems that mimic the complexity of nature.

One critical challenge facing the further development of DNA origami technology is to scale up the size of DNA origami structures. Herein we present a new strategy to construct 2D DNA origami of larger dimensions using rectangular-shaped DNA tiles as staple tiles rather than using traditional staple strands.

A small portion of the M13 scaffold (about 1140 nucleotides) is shown in Figure 1 to illustrate the concept.

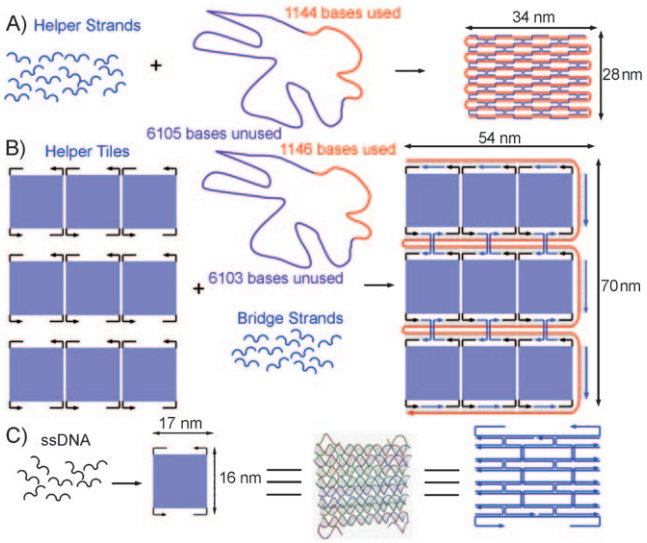

Figure 1. Experimental design. A) The formation of Rothemund's origami using many short staple strands to fold a single-stranded M13 DNA scaffold following a predetermined path into a closely packed 2D pattern. B) Formation of a larger-sized origami using a number of multihelical tiles, each containing single-stranded extensions at the four corners (short black lines; arrows indicate 3′ ends) as staple tiles, together with a number of bridge strands (blue) to fold the M13 DNA scaffold into a predetermined 2D structure. C) Self-assembly of the staple tiles, each being an 8-helix tile, 5 full helical turns long of about 17 nm × 16 nm. Each 8HX tile contains 18 strands of varying length, of which 16 strands remain unchanged, with two strands (one on the top and one on the bottom) extended with different sequences of single stranded overhangs to base-pair with different parts of the M13 strands.

Using Rothemund's original strategy, a segment of M13 can be folded by many short DNA staple strands into a rectangular shaped 2D origami of about 34 nm × 22 nm in dimension (Figure 1 A). In our new strategy (Figure 1 B), we use nine staple tiles, each of which is an eight-helix tile[24] (Figure 1 C) with protruding single-stranded overhangs at the four corners that base-pair with the M13 scaffold. Together with additional bridge strands, a segment of M13 of the same length can be folded into a fully packed 2D origami of circa 70 nm × 54 nm in two dimensions, which is more than quadruple the size of the structure shown in Figure 1 A. In principle, it is possible to use the staple-tile strategy to scale-up 2D DNA origami using the full-length M13 scaffold. This strategy may be further scaled up using larger staple tiles, such as a single tile of origami, to fold a longer scaffold strand (e.g. origami of origami).

[*] Z. Zhao, Prof. Dr. H. Yan, Prof. Dr. Y. Liu
Department of Chemistry and Biochemistry & The Biodesign Institute, Arizona State University
Tempe, AZ 85287 (USA)
Fax: (+1) 480-727-2378
E-mail: yan_liu@asu.edu
hao.yan@asu.edu

[**] This research was partly supported by grants from ONR, NSF, ARO to Y.L. and from ONR, ARO, NSF and Sloan Research Foundation to H.Y. Y.L. and H.Y. were supported as part of the Center for Bio-Inspired Solar Fuel Production, an Energy Frontier Research Center funded by the U.S. Department of Energy, Office of Science, Office of Basic Energy Sciences under Award Number DE-SC0001016.

Supporting information for this article is available on the WWW under http://dx.doi.org/10.1002/anie.200906225.

InterScience DISCOVER SOMETHING GREAT
© 2010 Wiley-VCH Verlag GmbH & Co. KGaA, Weinheim

As a proof-of-concept demonstration, we tested the construction of three fully packed 2D origami structures using altered numbers of staple tiles. The total numbers of tiles used in the three constructs are $5\times5=25$ (90 nm × 110 nm), $7\times8=56$ (140 nm × 200 nm), and $5\times11=55$ (100 nm × 280 nm). Additionally, a number of short bridge strands were used to guide the folding of the M13 scaffold into a flexible framework with correctly spaced cavities to facilitate access of the individual helper tiles to the scaffold. Single-stranded thymine, T2, was added at the ends of each helix to reduce inter-tile end-to-end base stacking. To minimize the cost of DNA synthesis, the core sequences of each individual eight-helix tile were kept the same, and only the DNA oligomers containing the overhangs that hybridize with the scaffold were modified. The scaffold used in the study was the single-stranded M13 mp18, (7249 nucleotides (nt) in length), same as that used in Rothemund's original origami experiments.[17] The final structures were designed so that 41%, 88%, or 90% of the scaffold strand were base-paired with the overhangs of the staple tiles and the bridge strands. The remaining scaffold was left as an unpaired loop at one side of the helices.

The formation of the three DNA origami structures using the staple-tile folding strategy were carried out in a two-step annealing procedure: 1) individual eight-helix staple tiles with unique overhangs at the four corners were annealed from 90 °C to 4 °C in 1xTAE-Mg buffer (pH 8.0), containing 20 mM Tris acetate, 1 mM EDTA, and 12.5 mM $Mg(OAc)_2$; in a separate tube, M13 scaffold strands and all of the bridge strands were annealed together in the same buffer conditions from 90 °C to 4 °C. 2) The above two solutions were mixed together and further annealed from 45 °C to 4 °C using various lengths of time to form the final structures. The molar ratio of the bridge strands to staple tiles to M13 scaffold was 10:2:1 for each assembly. The individual eight-helix tile has a melting temperature circa 65 °C,[24] so it should be stable at 45 °C. In our design, each individual eight-helix staple tile shares the same core sequence, so it is necessary to form the eight-helix tile first to prevent them from forming mismatched pairs with the M13 scaffold strand. The pre-annealing of the M13 scaffold strand with the bridge strands prepares the scaffold strand to pre-fold with a defined path, so that in the second annealing step, each individual staple tile can efficiently fill in the correctly spaced cavities along the scaffold to form the final target structure.

Folding of the 5×5 structure was quick and efficient. Complete 5×5 structures were observed with a 12 h thermal annealing from 45 °C to 4 °C. The formation of the 7×8 structure took a longer time. The correct folding was observed with annealing over the course of 60 h. The formation of the 5×11 structure was the least efficient process, with a limited yield even after 100 h of annealing.

The annealed mixtures were subjected to non-denaturing agarose gel electrophoresis (Figure 2, and Supporting Information, Figure S8) to check the yield of the target structures and purification. For the 5×5 structure, two distinct bands appeared that migrated more slowly than the M13 single strand. The relative intensities of these two bands showed no significant variation with an increase of the Mg^{2+} concentration from 12.5 mM to 20 mM with circa 1 mM increments. For the 7×8 and 5×11 structures, the agarose gel images (Figure 2B, and Supporting Information, Figure S8) showed one distinct slower migrating band. These two structures showed a higher yield with a moderately higher Mg^{2+} concentration (15 mM). It seems that this particular concentration of divalent cations aids the folding of the larger origami structures. From Figure 2 it appears that the M13 scaffold is fully consumed to form lower mobility structures. By measuring the relative intensity ratio of the target bands from the corresponding lane, excluding the faster migrating excessive helper tiles and bridge strands, the estimated yields are about 70% for the 5×5 structure (the lane used for AFM imaging) and circa 48% for the 7×8 structure. The bands (or smears) appeared above the target structures may come from misfolded products, as single stranded M13 scaffold may still contain some secondary structures at the initial temperature used (45 °C) in the second annealing step.

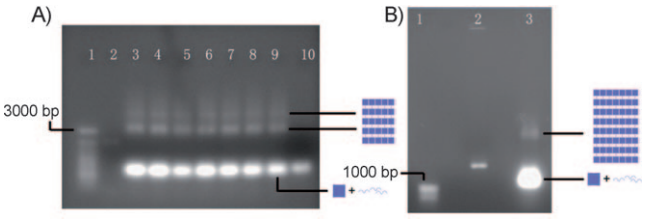

Figure 2. Agarose gel images that confirm the formation of the 5×5 and 7×8 structures. A) 5×5 structure. Lane 1: 100 bp marker ladder with a maximum marker size of 3000 bp; lane 2: single-stranded M13; lanes 3–9: annealed 5×5 structures at different Mg^{2+} concentrations (12.5 mM to 20 mM); lane 10: 8HX scaffold tiles. 0.7% agarose gel was used. B) 7×8 structure. Lane 1: 100 bp marker with a maximum marker size of 1000 bp; lane 2: single-stranded M13; lane 3: annealed mixture of 7×8 structure in 1.2xTAE-Mg buffer (15 mM Mg). 0.3% agarose gel was used. The gels were stained with ethidium bromide.

Both of the prominent slower migration bands for the 5×5 structure were excised from the gel and gently extracted using Freeze-N-Squeeze columns. The purified structures were then deposited on mica and imaged in liquid by tapping-mode atomic force microscopy (AFM). The AFM images (Figure 3A, see also the Supporting Information for more images) show that both the higher and lower bands contain complete or nearly complete assembly of the desired structure with no obvious differences. For this 5×5 structure, nearly 60% of the M13 sequence remains as a large flexible loop out of the structure. The two distinct bands might have resulted from a part of the M13 strand in the loop region breaking into a linear strand, thereby causing significant differences in the migration speeds of the structures in the gel.

AFM images (Figure 3) for the 5×5 and 7×8 structures reveal the correct folding of the designed structures using the staple tiles. Individual tiles of the correct dimension can be clearly distinguished in the images. The measured dimensions of the structures match the designed parameters. Both gel and AFM images demonstrate that the yield (or degree of completeness) of the final structure has a trend of $5\times5>7\times8$. It is logical that in a reaction with more components, a lower overall yield would be expected. We also noted that the

 © 2010 Wiley-VCH Verlag GmbH & Co. KGaA, Weinheim

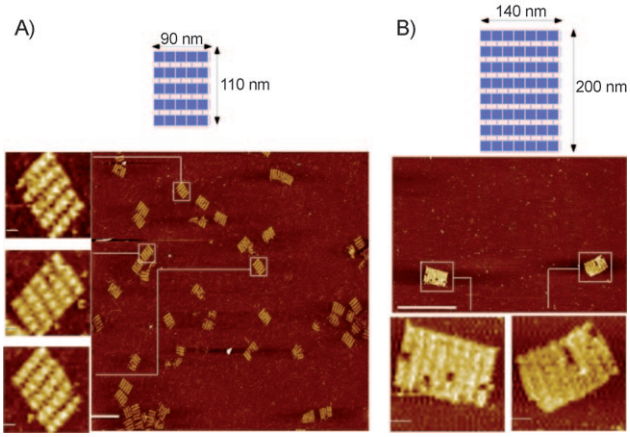

Figure 3. A) AFM images of the 5×5 structure. Scale bars in the insets are 20 nm. B) AFM pictures for the 7*8 structures. Scale bars in the insets are 40 nm. The yield of the desired structure is high, although the absence of one to three tiles at random positions is observed.

7×8 structure had a higher yield than the complete 5×11 structure, although they contain similar number of tiles in the assembly (56 tiles versus 55 tiles). This lower yield of the complete 5×11 structure (estimated to be about 30%; see the Supporting Information, Figure S8) may be explained by the larger aspect ratio of the final 5×11 structures (greater than 2:1, or even close to 3:1 when the stretching effect between the layers is considered), which resulted in unbalanced growth rates of the staple tiles in the vertical and lateral directions during the tile annealing. We tested the partial assembly of the 5×11 structure with various number of layers (8 to 11), and confirmed that fewer number of layers indeed gave better yields (see additional AFM images in the Supporting Information).

The 7×8 structure prepared here contains a single copy of the M13 strand, with a molecular weight of about 20 million Daltons, and circa 30000 base pairs. This is about four times the size of Rothemund's origami structure using the same length scaffold.[17] Because the core of the 8HX staple tiles was kept constant, the 16 strands were purified and used repeatedly in the assembly. The total number of DNA strands with a unique sequence remained a manageable size: 248, which is only a marginal increase from the original design of 226 strands used in the Rothemund's rectangular DNA origami.[17] As we used a two-step annealing strategy, it is foreseeable that we can selectively modify strands in each tile at particular positions and use them to create addressable binding sites to direct the assembly of other materials.

In summary, we have demonstrated a new strategy to scale up DNA origami using multihelical DNA tiles as folding staples. This strategy currently works more efficiently in creating 2D structures with roughly equal dimension in the 2D plane. The yield may be further improved by designing DNA staple tiles of different aspect ratios and optimizing the annealing procedures based on thermodynamic parameters of the helper tiles. In principle this method could be applied to create large DNA origami nanostructures reaching the size domain of conventional photolithography techniques (1 um), which may become a viable approach to bridge bottom up self-assembly with top-down lithography. For example, if the individual Rothemund rectangular 2D origami of 60×90 nm[17] were used as the staple tiles to fold a DNA scaffold of the size of λ DNA (45000 nucleotides, if a single strand of DNA of such length can be generated), it is possible to create super-origami of circa 10×8 of such tiles with an overall size of 1 um×0.5 um. Such super-origami should be easier to be patterned onto lithographically generated substrates. We anticipate the strategy demonstrated here could be combined together with other scale up techniques, such as hierarchical DNA assembly[18,19,25,26] or surface mediated self-assembly,[27,28] to realize the great potential of structural DNA nanotechnology.

Received: November 4, 2009
Revised: December 1, 2009
Published online: January 26, 2010

Keywords: DNA structures · protein folding · scanning probe microscopy · self-assembly

[1] N. C. Seeman, *Nature* **2003**, *421*, 427–431.
[2] F. A. Aldaye, A. L. Palmer, H. F. Sleiman, *Science* **2008**, *321*, 1795–1799.
[3] C. Lin, Y. Liu, H. Yan, *Biochemistry* **2009**, *48*, 1663–1674.
[4] F. C. Simmel, *Angew. Chem.* **2008**, *120*, 5968–5971; *Angew. Chem. Int. Ed.* **2008**, *47*, 5884–5887.
[5] C. M. Niemeyer, *Angew. Chem.* **2001**, *113*, 4254–4287; *Angew. Chem. Int. Ed.* **2001**, *40*, 4128–4158.
[6] H. Yan, S. H. Park, G. Finkelstein, J. H. Reif, T. H. LaBean, *Science* **2003**, *301*, 1882–1884.
[7] J. D. Le, Y. Pinto, N. C. Seeman, K. Musier-Forsyth, T. A. Taton, R. A. Kiehl, *Nano Lett.* **2004**, *4*, 2343–2347.
[8] J. Zheng, P. E. Constantinous, C. Micheel, A. P. Alivasatos, R. A. Kiehl, N. C. Seeman, *Nano Lett.* **2006**, *6*, 1502–1504.
[9] J. Sharma, R. Chhabra, A. Cheng, J. Brownbell, Y. Liu, H. Yan, *Science* **2009**, *323*, 112–116.
[10] J. Sharma, R. Chhabra, Y. Liu, Y. Ke, H. Yan, *Angew. Chem.* **2006**, *118*, 744–749; *Angew. Chem. Int. Ed.* **2006**, *45*, 730–735.
[11] Z. Deng, Y. Tian, S. H. Lee, A. E. Ribbe, C. Mao, *Angew. Chem.* **2005**, *117*, 3648–3651; *Angew. Chem. Int. Ed.* **2005**, *44*, 3582–3585.
[12] F. A. Aldaye, H. F. Sleiman, *Angew. Chem.* **2006**, *118*, 2262–2267; *Angew. Chem. Int. Ed.* **2006**, *45*, 2204–2209.
[13] O. Wilner, Y. Weizmann, R. Gill, O. Lioubashevski, R. Freeman, I. Willner, *Nat. Nanotechnol.* **2009**, *4*, 249–254.
[14] J. D. Cohen, J. P. Sadowski, P. B. Dervan, *Angew. Chem.* **2007**, *119*, 8102–8105; *Angew. Chem. Int. Ed.* **2007**, *46*, 7956–7959.
[15] A. Kuzuya, M. Kimura, K. Numajiri, N. Koshi, T. Ohnishi, F. Okada, M. Komiyama, *ChemBioChem* **2009**, *10*, 1811–1815.
[16] J. Malo, J. C. Mitchell, C. Venien-Bryan, J. R. Harris, H. Wille, D. J. Sherratt, A. J. Turberfield, *Angew. Chem.* **2005**, *117*, 3117–3121; *Angew. Chem. Int. Ed.* **2005**, *44*, 3057–3061.
[17] P. W. K. Rothemund, *Nature* **2006**, *440*, 297–302.
[18] S. M. Douglas, H. Dietz, T. Liedl, B. Hogberg, F. Graf, W. M. Shih, *Nature* **2009**, *459*, 414–418.
[19] H. Dietz, S. M. Douglas, W. M. Shih, *Science* **2009**, *325*, 725–730.
[20] Y. Ke, S. M. Douglas, M. Liu, J. Sharma, A. Cheng, A. Leung, Y. Liu, W. M. Shih, H. Yan, *J. Am. Chem. Soc.* **2009**, *131*, 15903–15908.
[21] Y. Ke, J. Sharma, M. Liu, K. Jahn, Y. Liu, H, Yan, *Nano Lett.* **2009**, *9*, 2445–2447.

 © 2010 Wiley-VCH Verlag GmbH & Co. KGaA, Weinheim

[22] E. S. Andersen, M. Dong, M. M. Nielsen, K. Jahn, R. Subramani, W. Mamdouh, M. M. Golas, B. Sander, H. Stark, C. L. P. Oliverira, J. S. Pedersen, V. Birkedal, F. Besenbacher, K. V. Gothelf, J. Kjems, *Nature* **2009**, *459*, 73 – 77.
[23] A. Kuzuya, M. Komiyama, *Chem. Commun.* **2009**, 4182 – 4184.
[24] Y. Ke, Y. Liu, J. Zhang, H. Yan, *J. Am. Chem. Soc.* **2006**, *128*, 4414 – 4421.
[25] S. H. Park, C. Pistol, S. J. Ahn, J. H. Reif, A. R. Lebeck, C. Dwyer, T. H. Labean, *Angew. Chem.* **2006**, *118*, 749 – 753; *Angew. Chem. Int. Ed.* **2006**, *45*, 735 – 739.
[26] C. Pistol, C. Dwyer, *Nanotechnology* **2007**, *18*, 125305 – 125309.
[27] X. Sun, S. H. Ko, C. Zhang, A. E. Ribbe, C. Mao, *J. Am. Chem. Soc.* **2009**, *131*, 13248 – 13249.
[28] S. Hamada, S. Murata, *Angew. Chem.* **2009**, *121*, 6952 – 6955; *Angew. Chem. Int. Ed.* **2009**, *48*, 6820 – 6823.

 © 2010 Wiley-VCH Verlag GmbH & Co. KGaA, Weinheim